PP2Ac knockdown attenuates lipotoxicity-induced pancreatic β-cell dysfunction and apoptosis

ZHENGWEI ZHANG[1], BEIER TONG[1], JIE LIU[1], JIEYUAN FENG[1], LINYANG SONG[1], HUAWEI WANG[1], MENGTING KE[1], CHENGKAI XU[2] and YANCHENG XU[1]

[1]Department of Endocrinology, Zhongnan Hospital of Wuhan University, Wuhan, Hubei 430071; [2]Department of Endocrinology, Suizhou Central Hospital, Suizhou, Hubei 441300, P.R. China

Received June 29, 2023; Accepted September 20, 2023

DOI: 10.3892/etm.2023.12247

Abstract. Protein phosphatase 2A (PP2A) is one of the most common serine/threonine phosphatases in mammalian cells, and it primarily functions to regulate cell signaling, glycolipid metabolism and apoptosis. The catalytic subunit of PP2A (PP2Ac) plays an important role in the functions of the protein. However, there are few reports on the regulatory role of PP2Ac in pancreatic β-cells under lipotoxic conditions. In the present study, mouse insulinoma 6 (MIN6) pancreatic cells were transfected with short hairpin RNAs to generate PP2Ac knockdown cells and incubated with palmitate (PA) to establish a lipotoxicity model. Serine/threonine phosphatase assay system, Cell Counting Kit-8, flow cytometry, enzyme-linked immunosorbent assay and western blotting were used to measure PP2A activity, cell viability, apoptosis, oxidative stress and insulin secretion in the cells. In addition, a mouse model of lipotoxicity was established with a high-fat diet (HFD) and the knockdown of PP2Ac using adeno-associated viruses to interfere with PP2Ac expression in the pancreatic tissues. The activity of PP2A in the mouse pancreatic tissue and the serum insulin level were measured. Furthermore, the proliferation of mouse pancreatic β-cells was assessed using pancreatic tissue immunofluorescence. PP2Ac knockdown inhibited lipotoxicity-induced PP2A hyperactivation, increased the resistance of pancreatic β-cells to lipotoxicity and attenuated PA-induced apoptosis in MIN6 cells. It also protected the endoplasmic reticulum and mitochondria, and ameliorated insulin secretion. The results of mRNA sequencing and western blotting analysis suggested that the protective effects of PP2Ac knockdown in MIN6 cells may be mediated via the MAPK pathway. Moreover, the results of the animal experiments suggested that specific knockdown of pancreatic PP2Ac effectively attenuated HFD-induced insulin resistance and reduced the compensatory proliferation of pancreatic β-cells in mice. In summary, the present study revealed the effects of interfering with PP2Ac gene expression on pancreatic β-cells *in vivo* and *in vitro* and the underlying mechanisms, which may provide insights for the treatment of type 2 diabetes mellitus in the clinic.

Correspondence to: Professor Chengkai Xu, Department of Endocrinology, Suizhou Central Hospital, 60 Longmen Street, Suizhou, Hubei 441300, P.R. China
E-mail: sinbasky@163.com

Professor Yancheng Xu, Department of Endocrinology, Zhongnan Hospital of Wuhan University, 169 Donghu Road, Wuhan, Hubei 430071, P.R. China
E-mail: xjl100901@whu.edu.cn

Abbreviations: AAV, adeno-associated virus; BSA, bovine serum albumin; CCK-8, Cell Counting Kit-8; ELISA, enzyme-linked immunosorbent assay; ER, endoplasmic reticulum; GSIS, glucose-stimulated insulin secretion; HFD, high-fat diet; IPGTT, intraperitoneal glucose tolerance test; KEGG, Kyoto Encyclopedia of Genes and Genomes; KRBB, Krebs-Ringer bicarbonate buffer; MIN6, mouse insulinoma 6; PA, palmitate; Pdx1, pancreatic and duodenal homeobox 1; PP2A, protein phosphatase 2A; PP2Ac, PP2A catalytic subunit; ROS, reactive oxygen species; SD, standard diet; TEM, transmission electron microscopy; TMRE, tetramethylrhodamine ethyl ester; T2DM, type 2 diabetes mellitus; UPR, unfolded protein response

Key words: PP2Ac, β-cell, lipotoxicity, dysfunction, apoptosis

Introduction

Alongside global development and population aging, the incidence of diabetes continues to increase annually (1). Data from the International Diabetes Federation suggest that ~537 million individuals were affected by diabetes in 2021, which constituted 10.5% of the global adult population, and this number is predicted to reach 783 million by 2045, representing 12.2% of the global adult population (2). Pancreatic β-cells play a vital role in sensing changes in the blood glucose concentration and releasing insulin in response to regulate it. The mechanism involves elevation of the ATP/ADP ratio, the closure of ATP-sensitive K^+ channels and activation of voltage-dependent Ca^{2+} channels (3,4). Multiple factors promote pancreatic β-cell dysfunction and apoptosis, resulting in their inability to produce sufficient insulin to control blood glucose levels, which is the main feature of type 2 diabetes mellitus (T2DM) (5). Previous studies have found that the incidence of T2DM increases linearly with the prevalence of obesity. This may be due to the greater quantity

of free saturated fatty acids in obese patients compared with patients of normal weight, which damages β-cell function, increases insulin resistance and destroys glucose homeostasis (6,7).

Under lipotoxic conditions, the unfolded protein response (UPR) is activated, which relieves endoplasmic reticulum (ER) stress by preventing protein translation, increasing the expression of chaperone proteins that perform refolding, and accelerating ER-associated degradation processes. However, sustained lipotoxic stimulation may cause the UPR to be unable to maintain ER homeostasis, resulting in the disruption of ER integrity followed by cell apoptosis (8-10). In addition, lipotoxicity increases the accumulation of mitochondrial reactive oxygen species (ROS) and induces mitochondrial DNA mutations, leading to mitochondrial dysfunction and impairing cellular energy metabolism (11). The impairment of mitochondrial function may play a key role in the development of insulin resistance (12). The ER and mitochondria are two of the most important organelles used by pancreatic β-cells to carry out their normal functions. The ER is crucial in insulin synthesis, proper folding of the insulin peptide and its response to glucose levels, while mitochondria produce ATP via glucose metabolism, which promotes the secretion of insulin (13,14).

Research to elucidate the mechanism by which lipotoxicity damages the function of the ER and mitochondria in pancreatic β-cells is urgently required. Palmitate (PA) is the most abundant saturated fatty acid in the body and is often employed to establish lipotoxicity models. It induces β-cell dysfunction and apoptosis through molecular mechanisms including oxidative stress, mitochondrial dysfunction and ER stress, thereby ultimately impairing glucose-stimulated insulin secretion (GSIS) (15,16).

Protein phosphatase 2A (PP2A) is a serine/threonine phosphatase consisting of a scaffolding A subunit, regulatory B subunit and catalytic C subunit. It is an important mediator of key cellular processes including glycosphingolipid metabolism, cell-cycle progression, signal transduction, protein translation, cell proliferation and cell apoptosis (17-19). The PP2A catalytic subunit (PP2Ac) mainly regulates the degree of substrate phosphorylation via its catalytic function and alters PP2A activity. The reduction of PP2A activity via the knockdown of PP2Ac has been shown to alleviate ER stress in cardiac and hepatic cells (20,21). In addition, high glucose levels have been demonstrated to disrupt mitochondrial integrity and function by modulating the pentose phosphate-PP2A pathway, thus resulting in mitochondrial disruption and altered mitochondrial respiration in hepatocytes (22). Furthermore, PP2Ac regulates insulin resistance in the liver and insulin secretion by pancreatic β-cells under conditions of glucose toxicity (23,24). However, the effects of PP2Ac on β-cell function, proliferation and apoptosis in a lipotoxic environment are not clear.

Therefore, the present study aimed to elucidate the role of PP2Ac knockdown in pancreatic β-cells exposed to lipotoxic conditions. The potential mechanism was evaluated in MIN6 cells and the effect of PP2Ac knockdown in pancreatic tissue on insulin resistance in a high-fat diet (HFD)-induced mouse model was examined.

Materials and methods

Cell culture. The mouse insulinoma 6 (MIN6) cell line was cultured in modified RPMI (cat. no. SH30809.01; HyClone; Cytiva) containing 10% (v/v) fetal bovine serum (cat. no. 10099-141; Gibco; Thermo Fisher Scientific, Inc.), 11.1 mM glucose, 2 mM L-glutamine and 1% penicillin/streptomycin in a humidified atmosphere with 5% CO_2 and 95% air at 37˚C. Cells were treated with PA or bovine serum albumin (BSA; cat. no. BS114-5g; Biosharp Life Sciences) at 37˚C in all experiments.

PP2A activity analysis. PP2A activity was measured using a Serine/Threonine Phosphatase Assay System (cat. no. V2460; Promega Corporation). Endogenous phosphate was removed by adding cell or tissue lysates to Sephadex® G-25 in Spin Columns provided with the kit. The treated samples and PP2A reaction buffer were added to a 96-well plate and incubated for 15 min at room temperature. The reaction was terminated by adding molybdate dye for 30 min and then measuring the optical density at 600 nm using a multifunctional plate reader (VICTOR® Nivo™; PerkinElmer, Inc.). A BCA Protein Assay Kit (cat. no. P0011; Beyotime Institute of Biotechnology) was used to calibrate the protein concentrations and calculate the relative activity of PP2A.

Generation of PP2Ac knockdown cells. Mouse PP2Ac gene (accession NM_019411) knockdown and negative control lentiviruses (plasmid backbone GV493) were designed and synthesized by Shanghai GeneChem Co., Ltd. MIN6 cells were cultured in a 6-well plate ($8x10^4$ cells/well), and when the degree of cell confluence reached ~30%, the PP2Acα-interfering or negative control lentiviruses (10 multiplicity of infection) were transfected into the cells, respectively. Stable PP2Ac knockdown cells and negative control groups were obtained after 48-72 h by screening with puromycin (13 μg/ml). The sequences of the three PP2Ac small hairpin RNAs (shRNAs) used for knockdown are listed in Table I. Three PP2Ac knockdown cell groups (sh1, sh2 and sh3) and a negative short hairpin control group (shc) were thereby constructed.

Reverse transcription-quantitative PCR (RT-qPCR). Transfected MIN6 cells were seeded in 6-well plates ($2x10^5$ cells/well) and cultured until the cell confluence reached 90%. Total RNA was extracted using an RNA extraction kit (cat. no. RN07; Aidlab Biotechnologies Co., Ltd.). RT was then conducted using the ReverTra Ace qPCR RT Kit (cat. no. FSQ101; Toyobo Life Science). The reaction steps were as follows: Pre-denaturation at 95˚C for 10 min, followed by 40 cycles of denaturation at 95˚C at 10 sec, annealing at 60˚C for 30 sec and extension at 72˚C for 30 sec. Relative expression changes were calculated using the $2^{-\Delta\Delta Cq}$ method (25). Finally, qPCR was performed using Magic SYBR Mixture (cat. no. CW3008M; CWBio) in a CFX96 RT-qPCR Detection System (Bio-Rad Laboratories, Inc.). β-actin mRNA was used as a control for the experiments. The sequences of the primers used for PCR were as follows: β-actin forward, 5'-GTGACGTTGACATCCGTAAAGA-3' and reverse, 5'-GTAACAGTCCGCCTAGAAGCAC-3'; and PP2Ac forward, 5'-ATGGACGAGAAGTTGTTCACC-3' and reverse, 5'-CAGTGACTGGACATCGAACCT-3'.

Table I. shRNA sequences.

shRNA	Sequence, 5'-3'
PP2Ac sh1	GAGACATTTAATCATGCCAAT
PP2Ac sh2	TTGACGACACTCTTAAGTATT
PP2Ac sh3	GACCGGAACGTAGTAACAATT
shc	TTCTCCGAACGTGTCACGT

PP2Ac, protein phosphatase 2A catalytic subunit; shRNA, short hairpin RNA; shc, shRNA negative control; sh1-3, shRNA 1-3.

ROS analysis. A master mix was prepared by dissolving dihydroethidium (cat. no. S0063; Beyotime Institute of Biotechnology) powder in DMSO to a concentration of 10 mM, and then diluted by 1:1,000 to reach the working solution concentration upon usage. MIN6 cells were seeded in 6-well plates ($2x10^5$ cells/well), cultured until cell confluence reached 60% and then treated with 0.5 mM PA or BSA for 24 h. The MIN6 cells were harvested by trypsinization and resuspended in 1 ml diluted working solution for 30 min at 37˚C. Next, the cells were washed three times with PBS and analyzed by the CytoFlex flow cytometry using the CytExpert software (version 2.4.0.28; Beckman Coulter, Inc.).

Mitochondrial membrane potential assay. Mitochondrial membrane potential was measured using tetramethylrhodamine ethyl ester (TMRE; cat. no. C2001S; Beyotime Institute of Biotechnology). MIN6 cells were seeded in 6-well plates ($2x10^5$ cells/well), cultured until cell confluence reached 60% and then treated with 0.5 mM PA or BSA for 24 h. Following treatment, the MIN6 cells were harvested by trypsinization and then incubated with PBS containing 10 nM TMRE for 30 min at 37˚C in the dark. The cells were washed with pre-warmed PBS and analyzed by the CytoFlex flow cytometry using the CytExpert software (version 2.4.0.28; Beckman Coulter, Inc.).

ATP measurement. ATP levels were measured using an ATP kit (cat. no. S0027; Beyotime Institute of Biotechnology). MIN6 cells were seeded in 6-well plates ($2x10^5$ cells/well) and cultured until cell confluence reached 60%, after which they were treated with 0.5 mM PA or BSA for 24 h. The cells were then lysed, and a supernatant was obtained via centrifugation at 12,000 x g for 5 min at 4˚C. A standard curve was established using an ATP standard solution. The working solution was prepared and the ATP concentration was measured using a VICTOR Nivo multipurpose microplate reader. To eliminate errors, the supernatant was collected for BCA protein quantification analysis to confirm its uniformity.

Determination of apoptosis. An Annexin V-APC/PI Apoptosis Detection Kit (cat. no. A30813; MultiSciences Biotech Co., Ltd.) was used to detect the cell apoptosis rate. MIN6 cells were seeded in 6-well plates ($2x10^5$ cells/well) and cultured until cell confluence reached 60%. Apoptosis was induced using 0.5 mM PA for 24 h at 37˚C, and BSA was used as a control. Annexin V-APC and PI dyes were added to the cell suspension, which was then incubated for 5 min at room temperature. Apoptosis was detected by the CytoFlex flow cytometry using the CytExpert software (version 2.4.0.28; Beckman Coulter, Inc.). Cells that were double positive for Annexin V and PI were considered late apoptotic cells, while cells that were Annexin V positive and PI negative were considered early apoptotic cells. The cell apoptosis rate was calculated as a percentage as follows: Sum of the number of cells at early and late apoptosis/total number of cells per well x100.

RNA sequencing. RNA was extracted and purified from PP2Ac knockdown and shc MIN6 cells, and a cDNA library was created using the NEBNext® Ultra™ RNA Library Prep Kit for Illumina® (cat. no. E7530L; New England Biolabs, Inc.). The insert size of the library was detected using a bioanalyzer (Agilent 2100; Agilent Technologies Co. Ltd.) to ensure the quality of the library. The effective concentration of the final library was >2 nM. Illumina sequencing (Illumina NovaSeq 6000; Illumina, Inc.) was performed with paired-end, and the end reading of 150 bp pairing was generated. The sequenced fragments were converted into sequencing data using a high-throughput sequencer to obtain raw reads. The filtered, clean reads were then compared with the reference genome (Mus Musculus: GRCm38/mm10) using the hisat2 software (version 2.0.5) (26) to obtain information on the positioning of the reads against the reference genome. The number of reads in the range from start to termination was calculated for each gene based on the information on the position of each gene pair against the reference genome. Finally, the differentially expressed genes were analyzed and Kyoto Encyclopedia of Genes and Genomes (KEGG) (27) pathway enrichment analysis was performed using the clusterProfiler software (version 3.8.1; Padj <0.05) (28). The RNA sequencing results are publicly available in the GEO database (accession number: GSE242538).

Insulin secretion assay. MIN6 cells were seeded in 6-well plates ($2x10^5$ cells/well), cultured until cell confluence reached 60% and then treated with 0.5 mM PA or BSA for 24 h. The cells were washed twice with Krebs-Ringer bicarbonate buffer (KRBB), sugar-free medium (cat. no. PM150122; Procell Life Science & Technology Co., Ltd.) was added and the cells were incubated for a further 30 min at 37˚C. KRBB solutions with 2.5 and 20 mM glucose were used to measure GSIS as previously described (24,29,30). The cells were incubated with these solutions for 2 h and the supernatants were obtained via centrifugation at 12,000 x g for 10 min at 4˚C. The insulin concentration was measured using a Mouse Insulin ELISA Kit (cat. no. E-EL-M2614c; Elabscience Biotechnology, Inc.). Relative insulin concentrations were calibrated by measurement of the protein concentration using the BCA method.

Cell viability determination. Cell Counting Kit-8 (CCK-8; cat. no. C0037; Biosharp Life Sciences) was used to measure cell viability. Cells were inoculated in 96-well plates at 6,000 cells/well and incubated in a cell culture incubator for 1 day. Different concentrations of PA were added, and the cells were further incubated for 24 h. Next, 10 μl CCK-8 working solution and 90 μl culture medium were added to each well and the plate was incubated for 2 h at 37˚C in the dark. Finally, the absorbance of each well was measured separately

using a VICTOR Nivo multifunctional microplate reader to calculate cell viability. When the appropriate concentration of PA was determined, this concentration was used for the assessment of cell viability using the aforementioned method at 12, 24, 36 and 48 h of incubation after the addition of PA, respectively.

Transmission electron microscopy (TEM). MIN6 cells were seeded in 10-cm cell culture dishes ($1x10^6$ cells/well) and cultured until cell confluence reached 60%. They were then treated with 0.5 mM PA or BSA for 24 h. Pre-chilled electron microscope stationary liquid (Wuhan Servicebio Technology Co., Ltd.) was added to fix the cells for 1 h at 4˚C, which were then sequentially dehydrated in a gradient of 50, 70, 80, 90, 95 and 100% ethanol. The cells were then embedded (1% agarose solution), sectioned (60 nm) and stained with 2% uranium acetate saturated alcohol solution and 2.6% lead citrate for 8 min at room temperature, respectively. Finally, images were analyzed by TEM (Hitachi, Ltd.).

Animal experiments. A total of 40 male 4-week-old C57BL/6J mice weighing ~20 g were purchased from SPF (Beijing) Biotechnology Co., Ltd. Mice were housed at constant temperature (22-26˚C) and humidity (50-60%), with a 12-h light/dark cycle during 1 week of adaptive feeding with free access to food and water. PP2Ac-interfering or control adeno-associated viruses (AAVs; Shanghai GeneChem Co., Ltd.) were respectively injected intraperitoneally into the mice at a final dose of $2.5x10^{11}$ viral genomes (vg) per mouse and expressed stably in the pancreas after 3 weeks. The AAV sequences are presented in Table II. The mice in the interfering and control groups were fed either a standard diet (SD; 0.2% fat, 71.5% carbohydrate and 18.3% protein; calorific value, 3.85 kcal/g) or HFD (61.6% fat, 20.3% carbohydrate and 18.1% protein; calorific value 5.24 kcal/g) for 12 weeks. The mice were finally divided into four groups: SD+AAV-null group, SD+AAV-PP2Ac group, HFD+AAV-null group and HFD+AAV-PP2Ac group, with 10 mice in each group. Fasting blood glucose was measured every 2 weeks. In addition, at the end of the 12-week feeding period and after a 16-h overnight fast, 2 g/kg glucose (25% glucose solution) was injected into the mice for the intraperitoneal glucose tolerance test (IPGTT). Blood glucose levels in the mice were measured using a glucometer (cat. no. AB-103G; Glucosure). After a further 3 days, the mice were anesthetized with 80 mg/kg 1% pentobarbital by intraperitoneal injection prior to blood collection from the orbital vein for serological testing. The mice were subsequently euthanized by CO_2 inhalation (flow rate, 40% of the chamber volume/min). The pancreas was removed by dissection, partially fixed in 4% paraformaldehyde solution, paraffin-embedded and histologically analyzed. The remainder of the pancreas was then frozen in liquid nitrogen and stored in a refrigerator at -80˚C for subsequent western blotting analysis. The animal experiments were approved by the Animal Ethics and Experimentation Committee of Wuhan University (approval no. ZN2022037).

Analysis of glucose tolerance and serum parameters in mice. Every 2 weeks the mice were fasted overnight for 16 h and their fasting blood glucose was measured the following day. The IPGTT was performed by injecting glucose into the mice intraperitoneally at a dose of 2 g/kg and measuring the blood glucose levels of the mice at 15, 30, 60 and 120 min using a glucometer. In addition, plasma was isolated from the blood collected from the orbital vein of the mice at the end of the experiment. The serum levels of triglycerides and total cholesterol were analyzed using kits (cat. nos. A110-H and A111-1-1, respectively; Nanjing Jiancheng Bioengineering Institute) according to the manufacturer's instructions. Serum insulin levels were measured using ELISA kits (cat. no. E-EL-M2614c; Elabscience Biotechnology, Inc.).

Table II. AAV sequences.

AAV	Sequence, 5'-3'
AAV-null	TTCTCCGAACGTGTCACGT
AAV-PP2Ac	TTGACGACACTCTTAAGTATT

AAV, adeno-associated virus; AAV-null, AAV vector with a null transgene; AAV-PP2Ac, AAV vector with PP2Ac transgene knockdown.

Analysis of islet β-cell area and proliferation rate in mice. After euthanizing each mouse, the pancreas was removed, washed twice with PBS and fixed in 4% paraformaldehyde solution at room temperature. After paraffin embedding and sectioning (4 μm), the pancreas was treated with xylene and different concentrations of ethanol prior to dewaxing and dehydration. After blocking with 5% BSA at room temperature for 30 min, primary antibodies against Ki67 (1:200 dilution; cat. no. GB121141-100; Wuhan Servicebio Technology Co., Ltd.) and insulin (1:200; cat. no. A19066; ABclonal Biotech Co., Ltd.) were added to the sections and incubated overnight at 4˚C. The next day, secondary antibodies conjugated to the fluorescent dyes FITC (1:100; cat. no. GB22303; Wuhan Servicebio Technology Co., Ltd.) and Cy3 (1:100; cat. no. GB21301; Wuhan Servicebio Technology Co., Ltd.) were incubated with the sections at room temperature for 1 h. The nuclei were then stained with DAPI reagent at room temperature for 5 min in the dark before being observed under a fluorescence microscope and photographed. FITC-labeled insulin appeared green, while Cy3-labeled Ki67 appeared red and nuclei stained by DAPI appeared blue. The β-cell proliferation rate was calculated as the proportion of cells positive for Ki67 labeling among the number of insulin-positive cells. Cell counting and fluorescence intensity quantification were performed using ImageJ software (version 1.42; National Institutes of Health).

Western blotting analysis. Pancreatic tissue or MIN6 cells were homogenized with RIPA lysis buffer (cat. no. P0013B; Beyotime Institute of Biotechnology) containing protease inhibitors. The supernatant was then obtained via centrifugation at 12,000 x g for 20 min at 4˚C and the total protein in the supernatant was quantified with a BCA kit. Equal protein quantities were separated by 12.5% SDS-PAGE and transferred to PVDF membranes (Millipore; cat. no. IPVH00010; Sigma-Aldrich (Shanghai) Trading

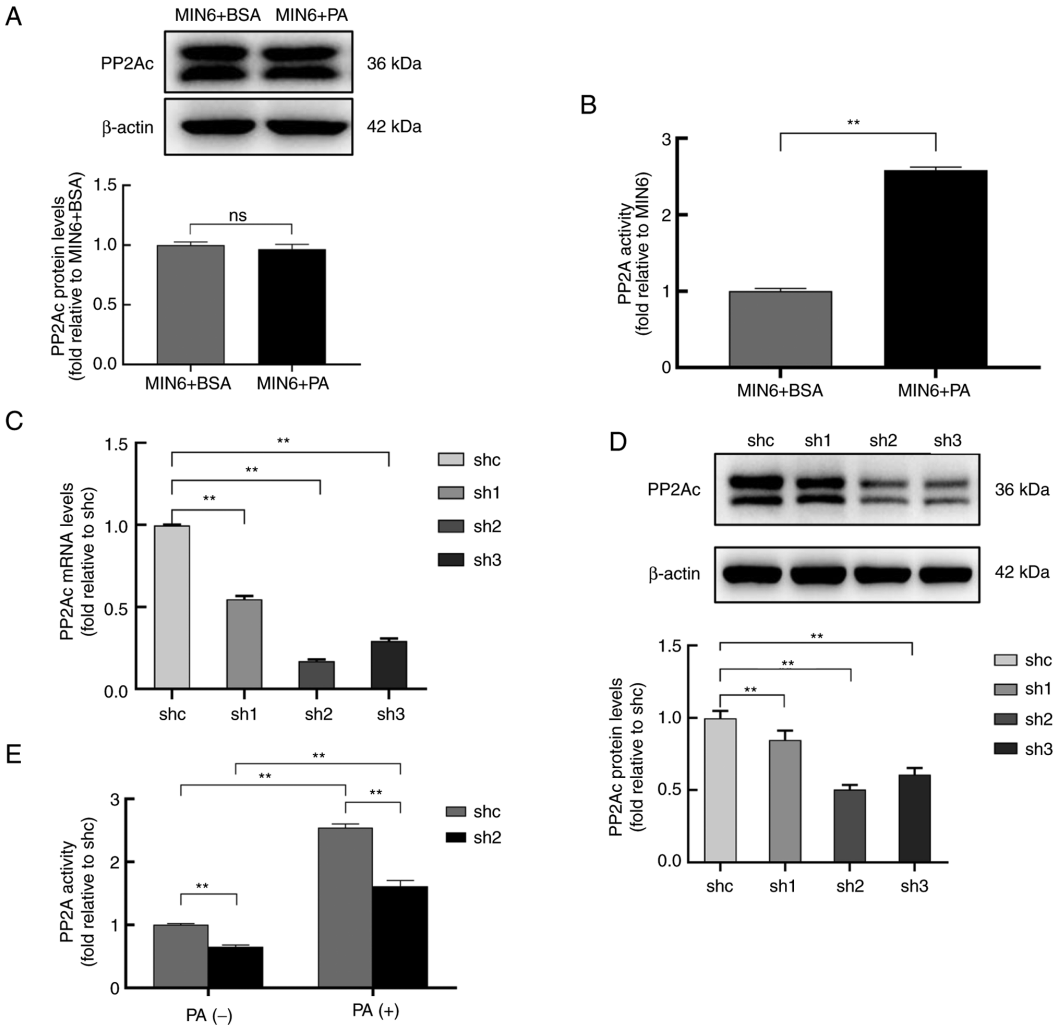

Figure 1. Knockdown of PP2Ac in MIN6 cells significantly attenuates PA-induced PP2A hyperactivation. MIN6 cells were treated with 0.5 mM BSA or PA for 24 h, and (A) PP2Ac protein levels and (B) PP2A activity were assayed. (C) RNA was isolated from MIN6 cells in three PP2Ac knockdown cell groups and PP2Ac transcript levels were assessed by reverse transcription-quantitative PCR using β-actin as the reference gene. (D) The PP2Ac protein levels of the transfected MIN6 cells were analyzed by western blotting using β-actin as a loading control. (E) PP2Ac knockdown and control MIN6 cells were treated with 0.5 mM BSA or PA for 24 h and PP2A activity was measured. All experiments were performed at least three times, and values are reported as the mean ± standard deviation. **P<0.01. PP2Ac, catalytic subunit of protein phosphatase 2A; MIN6, mouse insulinoma 6; PA, palmitate; BSA, bovine serum albumin; shc, short hairpin RNA control; sh1-3, PP2AC short hairpin RNAs 1-3; ns, not significant.

Co., Ltd.). After blocking the membranes with 5% skimmed milk at room temperature for 2 h, they were incubated with primary antibodies at 4˚C overnight. The following day, the membranes were washed and incubated with secondary antibodies at room temperature for 1 h. The primary antibodies used were as follows: Anti-β-actin (1:50,000; cat. no. 66009-1-Ig; Proteintech Group, Inc.), anti-PP2Ac (1:2,000; cat. no. 2259s; CST Biological Reagents Co., Ltd.), anti-microtubule-associated protein 1 light chain 3 b (LC3B; 1:2,000; cat. no. A19665;), anti-glucose-regulated protein 78 (GRP78; 1:2,000; cat. no. A4908), anti-CHOP (1:2,500; cat. no. A0221), anti-caspase 3 (1:2,000; cat. no. A19654), anti-Bcl-2 (1:2,000; cat. no. A19693), anti-Bax (1:2,000; cat. no. A19684), anti-pancreatic and duodenal homeobox 1 (Pdx1; 1:2,000; cat. no. A3070) and anti-insulin (1:2,000; cat. no. A19066), all from ABclonal Biotech Co., Ltd. β-actin was used as a control for normalization. Additional primary antibodies were used to detect cellular signaling pathways, as follows: Anti-ERK1/2 (1:2,000 dilution; cat. no. A16686), anti-phosphorylated (p)-ERK1/2 (1:2,000; cat. no. AP0472), anti-JNK (1:2,000; cat. no. A4867), anti-p-JNK (1:2,000; cat. no. AP0631), anti-p38 (1:2,000; cat. no. A0227), anti-p-p38 (1:2,000; cat. no. AP0057) and anti-β-tubulin (1:1,000; cat. no. A0021), all from ABclonal Biotech Co., Ltd. β-tubulin was used as a control for normalization. Secondary antibodies conjugated to horseradish peroxidase were used as follows: Goat anti-rabbit (1:5,000 dilution; cat. no. AS014; ABclonal Biotech Co., Ltd.) and goat anti-mouse (1:5,000; cat. no. AS003; ABclonal Biotech Co., Ltd.). Immunoreactive bands were visualized with an automatic chemiluminescence image analysis system (Tanon 5200; Tanon Science and Technology Co., Ltd.), and the grayscale values of proteins were analyzed with ImageJ software (version 1.53e).

Statistical analysis. All results are expressed as the mean ± standard deviation and were analyzed using the SPSS 20.0 software package (IBM Corp.). Graphs were plotted

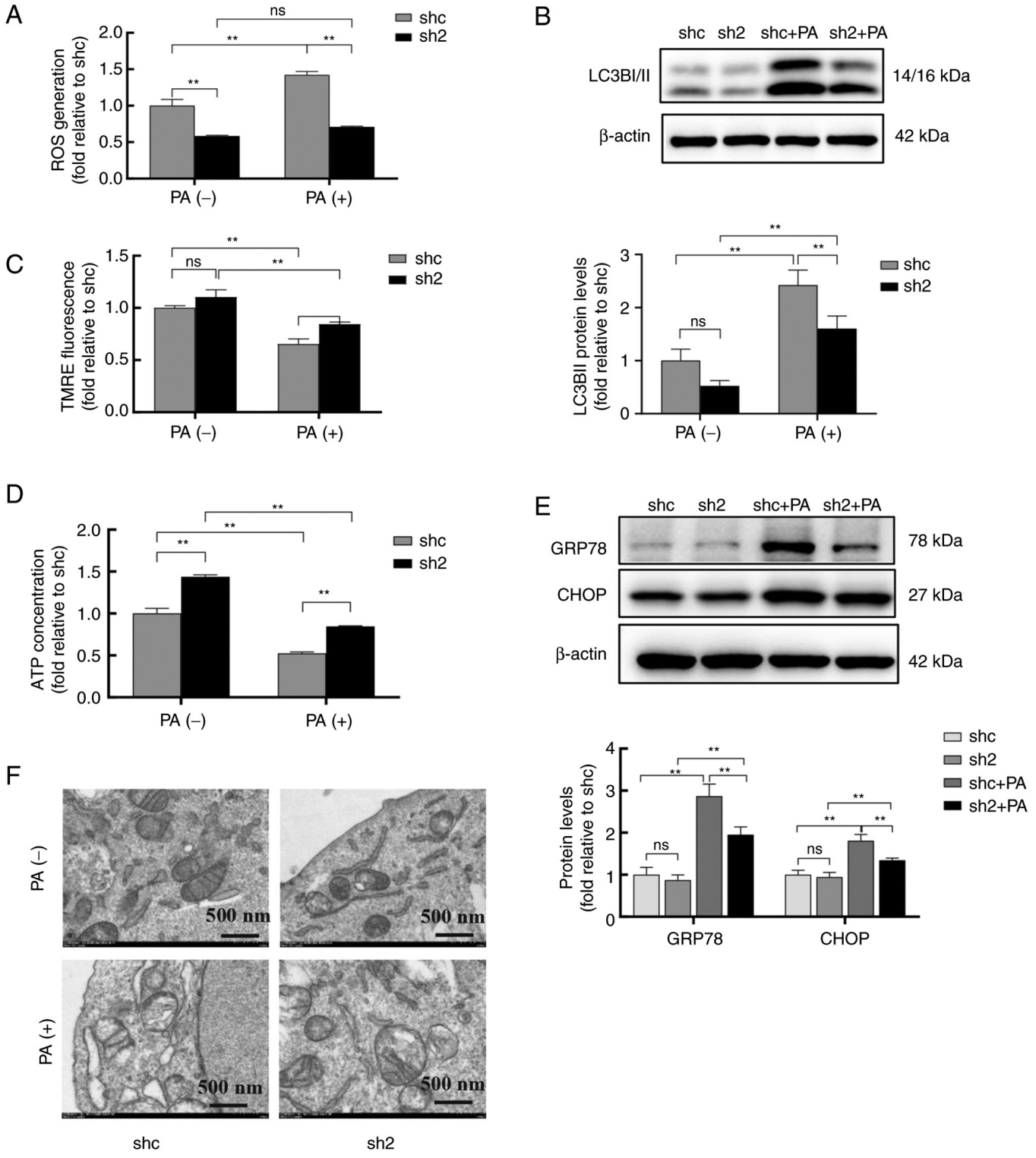

Figure 2. PP2Ac knockdown alleviates PA-induced mitochondrial dysfunction and endoplasmic reticulum stress in MIN6 cells. MIN6 cells with or without PP2A knockdown were treated with 0.5 mM bovine serum albumin or PA for 24 h. (A) Cellular ROS levels were detected by labeling with dihydroethidium probe and analysis by flow cytometry. (B) Protein levels of LC3BI/II were analyzed by western blotting in MIN6 cells, and β-actin was used as a loading control. (C) Mitochondrial membrane potential was measured by flow cytometry using TMRE dye. (D) ATP levels of the transfected cells were quantified. (E) Protein expression levels of GRP78 and CHOP were analyzed by western blotting in MIN6 cells, and β-actin was used as a loading control. (F) Transmission electron microscopy was used to observe the ultrastructure of the mitochondria and ER in MIN6 cells. All experiments were performed at least three times, and values are reported as the mean ± standard deviation. **P<0.01. PP2Ac, catalytic subunit of protein phosphatase 2A; PA, palmitate; MIN6, mouse insulinoma 6; ROS, reactive oxygen species; LC3BI/II, microtubule-associated protein 1 light chain 3 b I/II; TMRE, tetramethylrhodamine ethyl ester; GRP78, glucose-regulated protein 78; shc, short hairpin RNA control; sh2, PP2AC short hairpin RNA 2; ns, not significant.

using GraphPad Prism 8 (GraphPad Software; Dotmatics). Statistically significant differences between two experimental conditions were analyzed with the paired Student's t-test. Comparisons between multiple groups with single independent

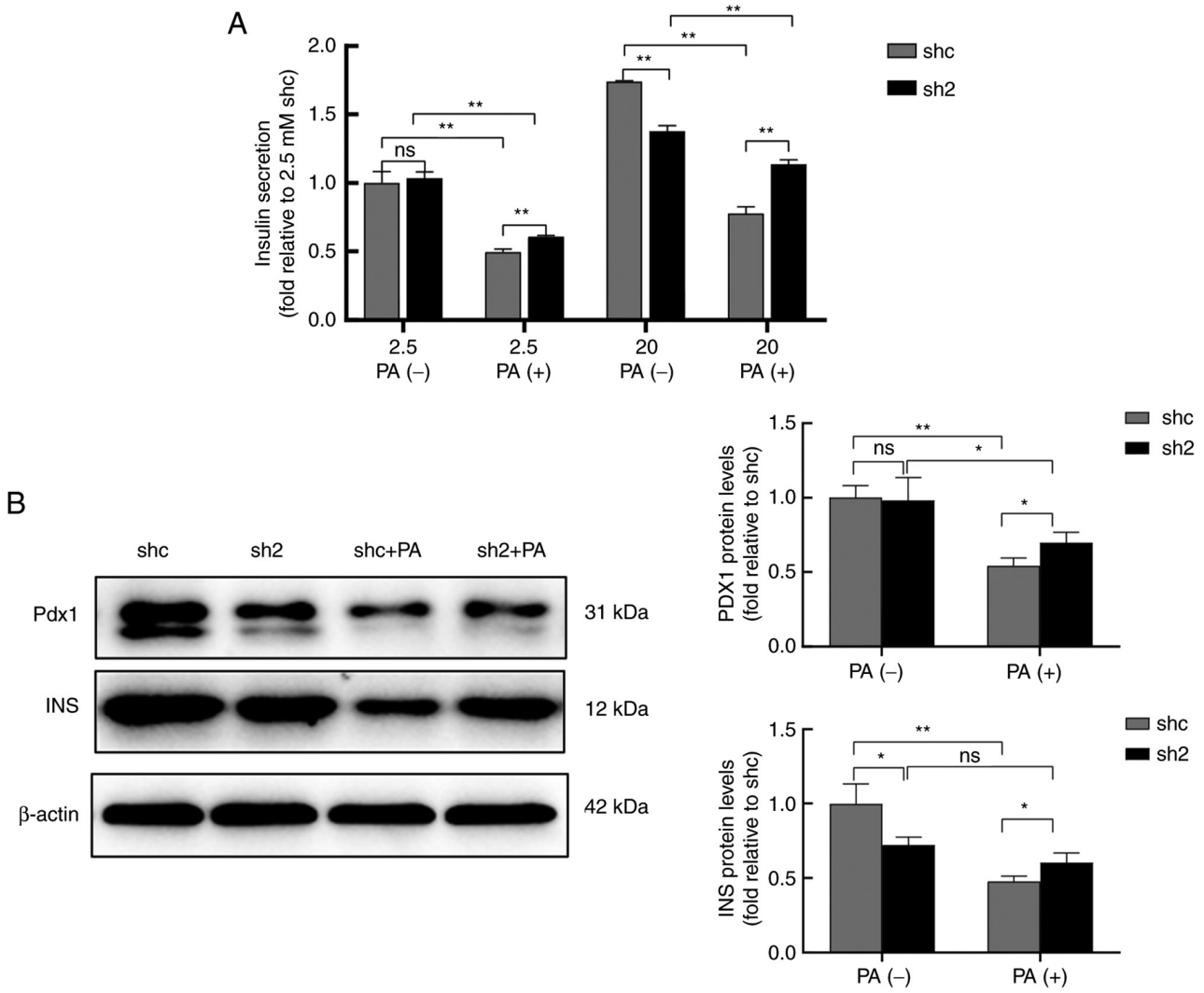

Figure 3. PP2Ac knockdown increases the secretion of INS by MIN6 cells under PA exposure. (A) INS secretion of MIN6 cells with or without PP2Ac knockdown stimulated by low glucose (2.5 mM) and high glucose (20 mM). (B) Expression levels of the INS secretion-associated proteins Pdx1 and INS were analyzed by western blotting, and β-actin was used as a loading control. All experiments were performed at least three times, and values are reported as the mean ± standard deviation. *P<0.05, **P<0.01. PP2Ac, catalytic subunit of protein phosphatase 2A; INS, insulin; MIN6, mouse insulinoma 6; PA, palmitate; Pdx1, pancreatic and duodenal homeobox 1; shc, short hairpin RNA control; sh2, PP2AC short hairpin RNA 2; ns, not significant.

variable were analyzed by one-way ANOVA followed by Tukey's post hoc test, while those with two independent variables were analyzed by two-way ANOVA with Bonferroni correction. P<0.05 was considered to indicate a statistically significant difference.

Results

Knockdown of PP2Ac in MIN6 cells significantly attenuates PA-induced PP2A hyperactivation. To assess the PP2A status in MIN6 cells under lipotoxic conditions, MIN6 cells were treated with 0.5 mM BSA or PA for 24 h, and the PP2Ac protein expression level and PP2A activity of the cells were assayed. The data in Fig. 1A and B indicate that PA exposure significantly activated PP2A, although it did not change the protein expression level of PP2Ac in the MIN6 cells. Three PP2Ac knockdown cell groups and a shc control group were constructed by the transfection of MIN6 cells with lentiviral vectors. The results showed that, compared with those in the shc group, the mRNA levels of PP2Ac for sh1, sh2 and sh3 were reduced to 55, 17 and 19%, respectively (Fig. 1C), while the PP2Ac protein expression levels were reduced to 85, 50 and 61%, respectively (Fig. 1D). As the sh2 cell line exhibited the greatest knockdown effect, it was selected for the analysis of PP2A activity under lipotoxic conditions. The results showed that the knockdown of PP2Ac in MIN6 cells significantly attenuated PA-induced PP2A hyperactivation (Fig. 1E).

PP2Ac knockdown alleviates PA-induced mitochondrial dysfunction and ER stress in MIN6 cells. Mitochondria and the ER are crucial organelles for insulin synthesis and secretion in pancreatic β-cells. Therefore, the effects of PP2Ac knockdown using shRNAs on the function and morphology of mitochondria and the ER were studied in MIN6 cells under lipotoxic conditions. The results revealed that PA significantly increased endogenous ROS generation and LC3BII protein expression levels, and decreased the mitochondrial membrane potential

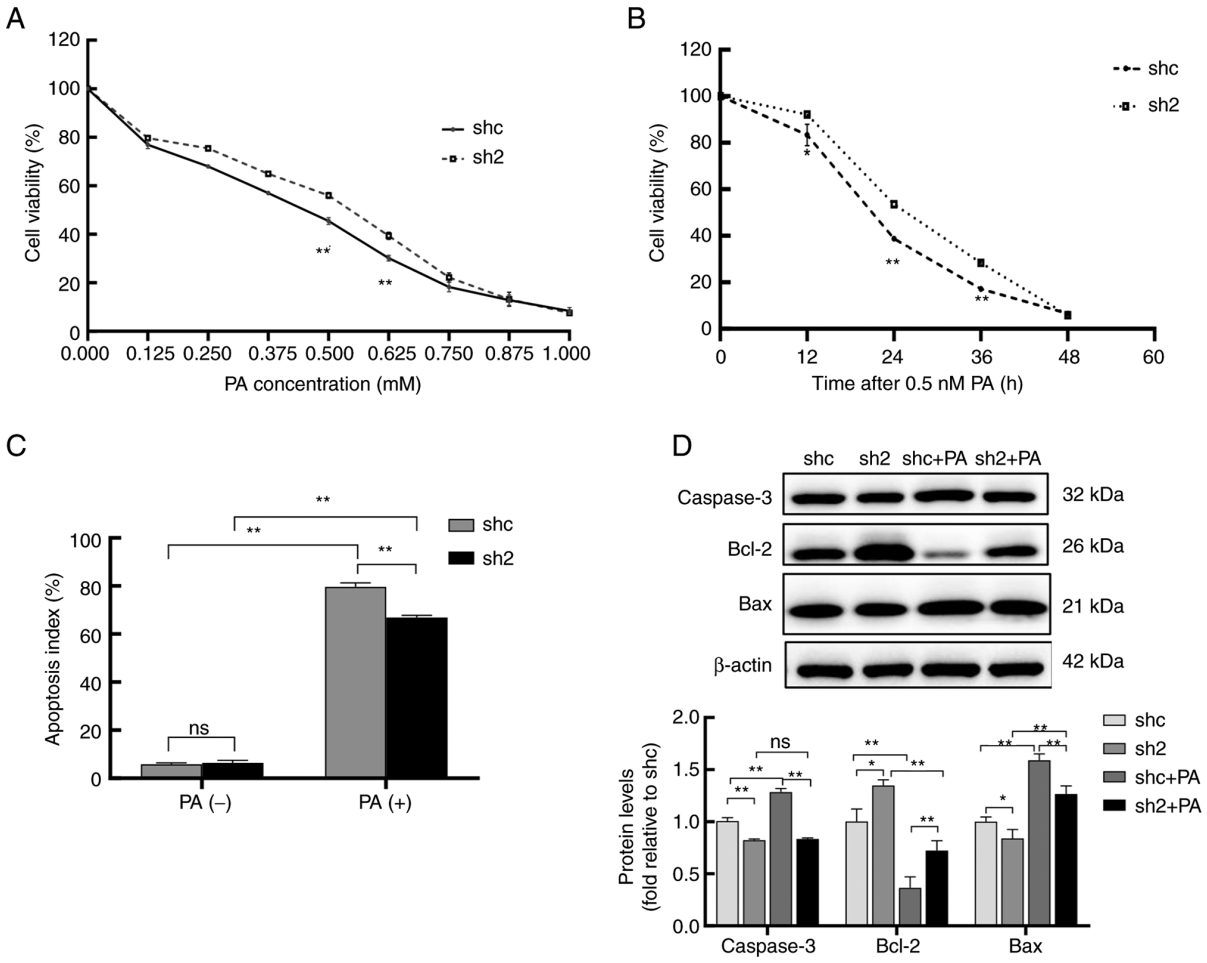

Figure 4. PP2Ac knockdown attenuates PA-induced apoptosis in MIN6 cells. (A) PP2Ac knockdown increases the resistance of MIN6 cells to PA; cell viability decreased following the addition of various concentrations of PA, but the decline in viability was less in the sh2 group than in the shc group. (B) Exposure of the cells to 0.5 mM PA for 12, 24, 36 and 48 h, reduced cell viability, but the cell viability of the sh2 group was always higher than that of the shc group. (C) Apoptosis of the MIN6 cells was detected by flow cytometry. (D) Expression levels of the apoptosis-associated proteins caspase 3, Bcl-2 and Bax in the transfected MIN6 cells were analyzed by western blotting, using β-actin as a loading control. All experiments were performed at least three times, and values are reported as the mean ± standard deviation. *P<0.05, **P<0.01. PP2Ac, catalytic subunit of protein phosphatase 2A; PA, palmitate; MIN6, mouse insulinoma 6; shc, short hairpin RNA control; sh2, PP2AC short hairpin RNA 2; ns, not significant.

and ATP levels of the cells, whereas PP2Ac knockdown significantly alleviated these effects (Figs. 2A-D, S1 and S2).

GRP78 and CHOP are typical markers of ER stress. After exposure to PA, the protein levels of GRP78 and CHOP were significantly increased in both the shc and sh2 groups. However, in the PA-treated cells, the protein levels of GRP78 and CHOP were lower in the cells transfected with sh2 compared with those transfected with shc (Fig. 2E). The ultrastructures of the mitochondria and ER in MIN6 cells were observed using TEM (Fig. 2F). The TEM images revealed that exposure to PA promoted mitochondrial swelling and rupture, and the disappearance of mitochondrial ridges, while it decreased the quantity of the ER, all of which were markedly alleviated in the MIN6 cells with PP2Ac knockdown. These results suggest that PP2Ac knockdown alleviates PA-induced mitochondrial dysfunction and ER stress in MIN6 cells.

PP2Ac knockdown increases insulin release in MIN6 cells under PA exposure. Insulin secretion under low glucose (2.5 mM) and high glucose (20 mM) conditions was examined. PA significantly reduced insulin secretion when stimulated with both low and high glucose concentrations, while PP2Ac knockdown effectively increased insulin secretion (Fig. 3A). After exposure to 0.5 mM PA, the protein expression levels of insulin and Pdx1, which are associated with insulin secretion, were reduced in MIN6 cells, but PP2Ac knockdown effectively alleviated these reductions (Fig. 3B). These results suggest that PP2Ac knockdown protected the insulin secretory function of MIN6 cells against the effects of PA exposure, which may indicate that the knockdown of PP2Ac is associated with enhanced resistance to lipotoxicity in MIN6 cells.

PP2Ac knockdown attenuates PA-induced apoptosis in MIN6 cells. CCK-8 analysis revealed that the cell viability of the sh2 group was markedly lower than that of the shc group at different concentrations of PA and durations of exposure (Fig. 4A and B). PA increased the apoptosis rate of MIN6 cells compared with that of the untreated control cells, while the knockdown of PP2Ac effectively inhibited the PA-induced increase in the apoptosis rate (Figs. 4C and S3). Previous studies have shown that caspase 3, Bcl-2 and Bax are important factors in the endogenous signaling pathway underlying

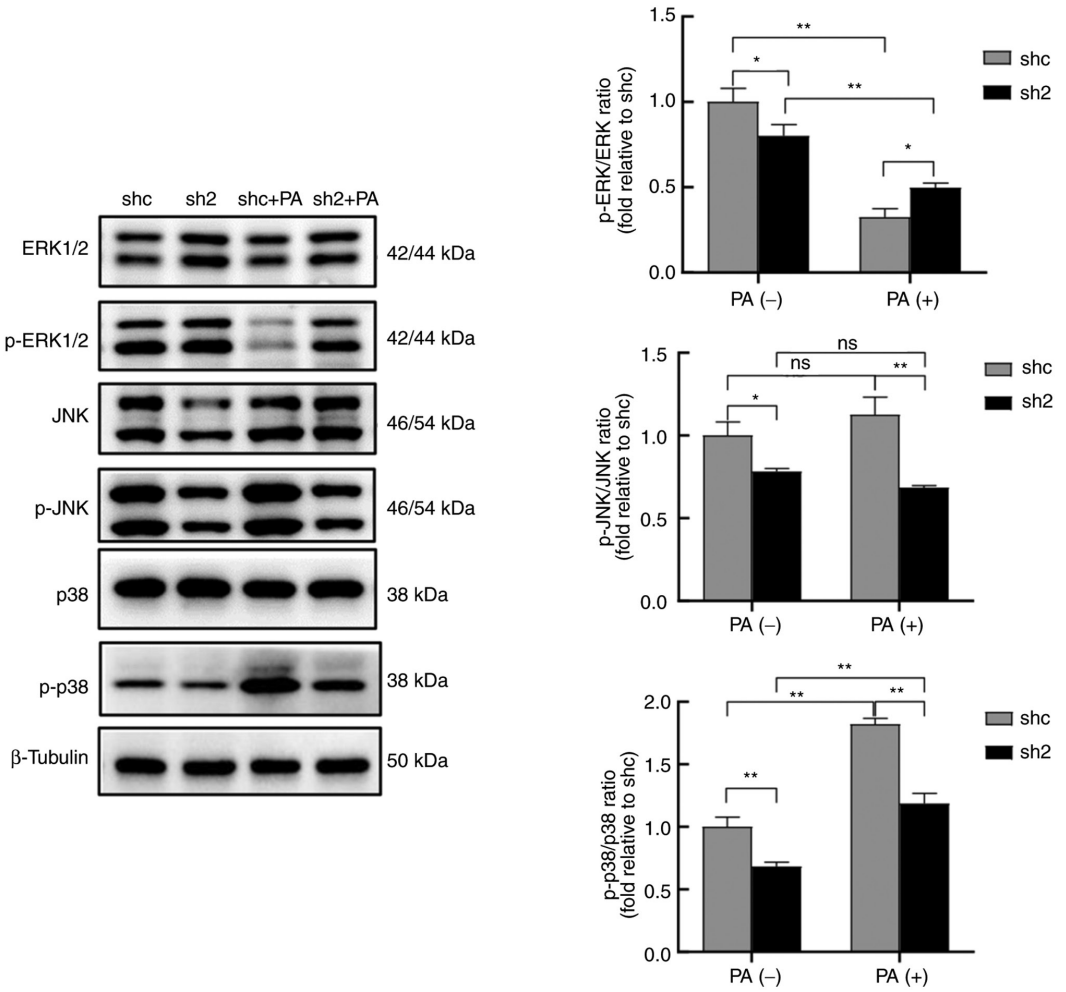

Figure 5. PP2Ac knockdown is associated with changes to the MAPK pathway in MIN6 cells under lipotoxic conditions. Protein expression and phosphorylation levels of ERK, JNK and p38 MAPK pathway proteins in MIN6 cells with or without PP2Ac knockdown were analyzed by western blotting, using β-tubulin as a loading control. The ratios of p-ERK/ERK, p-JNK/JNK, p-p38/p38 was analyzed. All experiments were performed at least three times, and values are reported as the mean ± standard deviation. *P<0.05, **P<0.01. PP2Ac, catalytic subunit of protein phosphatase 2A; MIN6, mouse insulinoma 6; PA, palmitate; shc, short hairpin RNA control; sh2, PP2AC short hairpin RNA 2; p-, phosphorylated; ns, not significant.

apoptosis (31). Western blotting revealed that caspase 3 and Bax protein levels were increased, while those of Bcl-2 were decreased, in MIN6 cells after PA exposure. Compared with those in the shc cells, the PA-induced changes of protein expression were alleviated in MIN6 cells with PP2Ac knockdown (Fig. 4D). These results suggest that PP2Ac knockdown increased the resistance of MIN6 cells to PA and reduced apoptosis, which may be associated with inhibition of the endogenous apoptotic pathway.

PP2Ac knockdown is involved in MAPK pathway changes under lipotoxicity. Sequencing analysis revealed that PP2Ac knockdown resulted in the upregulation of 1,332 genes and the downregulation of 1,707 genes compared with those in the shc group. Based on the results of the KEGG pathway enrichment analysis, the MAPK signaling pathway was selected for validation (Figs. S4 and S5). Although no significant difference in the MAPK signaling pathway was detected by mRNA sequencing analysis, a difference at the protein level was revealed by western blot analysis; it must be noted that the MIN6 cells were not treated with PA before sequencing. Western blotting demonstrated that ERK protein levels were unaffected by PA exposure in both the shc and sh2 cells, while the PP2Ac knockdown groups exhibited higher protein levels of ERK than the respective shc groups. Importantly, PP2Ac knockdown effectively alleviated the reduction in the phosphorylation levels of ERK caused by PA. Although some changes in JNK expression were observed, p38 protein levels did not change significantly in any group following PA treatment or PP2Ac knockdown, while PP2Ac knockdown attenuated p-JNK levels and the increase in p-p38 levels induced by PA (Fig. 5). Overall, the results indicate that PP2Ac knockdown attenuated PA-induced apoptosis, and this may have occurred through the activation of ERK via the MAPK signaling pathway, and inhibition of the JNK and p38 pathways.

AAVs interfere with PP2Ac gene expression in mice to improve their metabolic function. To investigate the effect of the PP2Ac gene on β-cell function in mice, the expression of the PP2Ac gene was specifically disrupted in pancreatic tissue using an AAV, and mice were fed with either an SD or a HFD for 12 weeks. Western blotting results showed that the protein levels of PP2Ac were successfully reduced in the pancreatic tissues of mice injected with AAV-PP2Ac, and

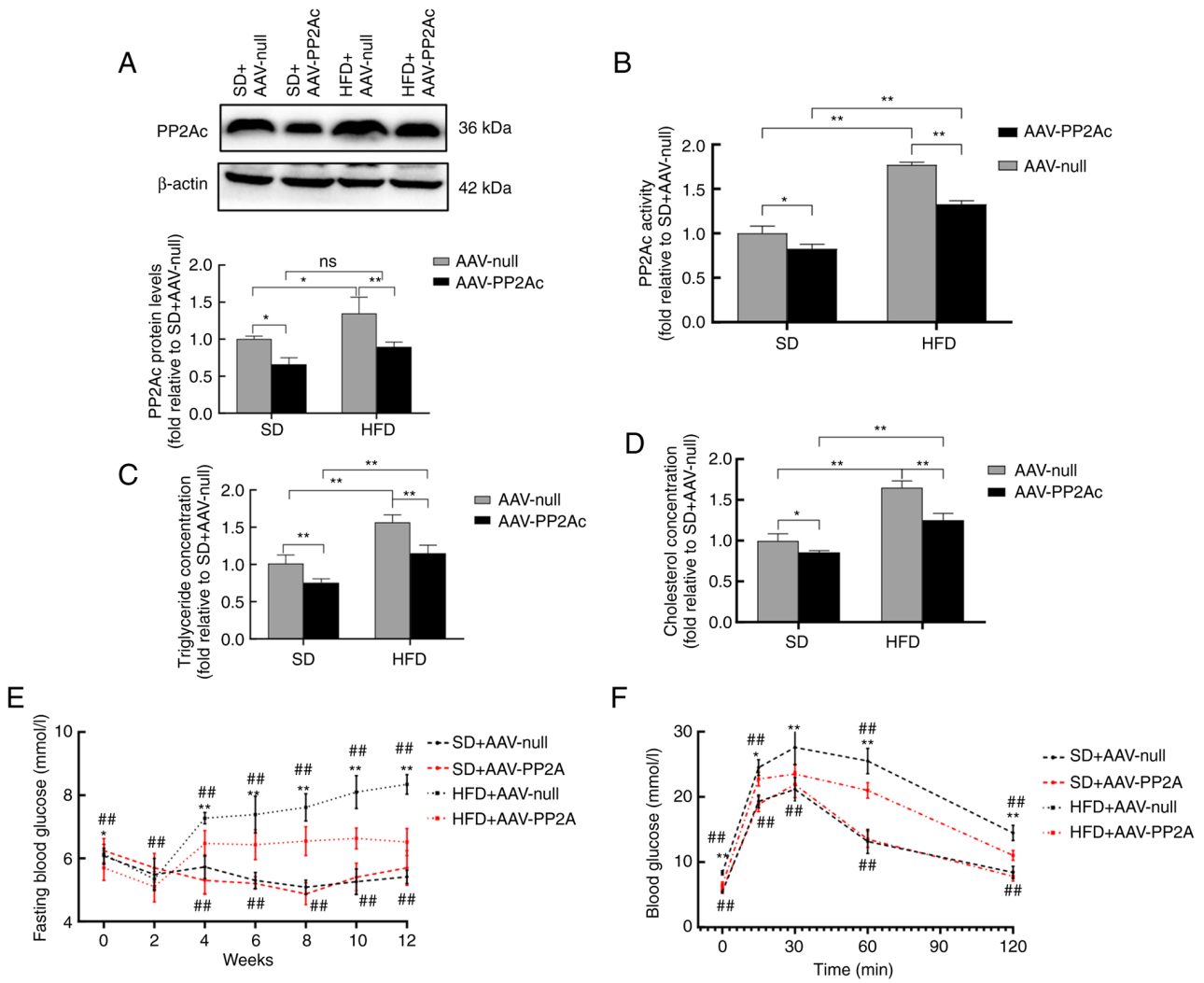

Figure 6. AAVs interfere with PP2Ac gene expression in mice and improve their metabolic function. (A) PP2Ac protein expression levels of mouse pancreatic tissues were analyzed by western blotting, using β-actin as a loading control. (B) PP2A activity was also assayed in the pancreatic tissues. Mouse serum was isolated, and (C) triglycerides (n=5) and (D) cholesterol (n=5) concentrations were measured. *P<0.05, **P<0.01. (E) Fasting blood glucose levels in the mice were measured every 2 weeks (n=7) and (F) glucose tolerance was measured at the end of the 12-week feeding period (n=7). *P<0.05, **P<0.01 for AAV-null vs. AAV-PP2Ac (same dietary conditions); $^{\#\#}$P<0.01 for SD vs. HFD (same AAV). All experiments were performed at least three times, and values are reported as the mean ± standard deviation. AAV, adeno-associated virus; PP2Ac, protein phosphatase 2A; SD, standard diet; HFD, high-fat diet.

AAV-PP2Ac significantly inhibited the PP2A activation triggered by HFD feeding (Fig. 6A and B). HFD feeding increased the serum cholesterol and triglyceride levels in mice, while AAV-PP2Ac treatment reduced the extent of these elevations (Fig. 6C and D). Fasting blood glucose was measured every 2 weeks in the mice, and the results revealed that HFD-induced hyperglycemia started in the fourth week, while HFD-fed mice in the AAV-PP2Ac group maintained lower levels than those in the AAV-null group (Fig. 6E). In addition, the IPGTT showed that mice in the AAV-PP2Ac group had improved glucose tolerance compared with those in the AAV-null group with HFD feeding (Fig. 6F). These results indicate that HFD feeding activated PP2A in the pancreatic tissue, leading to metabolic disorder and impaired glucose metabolism in mice, while the knockdown of pancreatic PP2Ac ameliorated these outcomes.

Interference with the PP2Ac gene attenuates the HFD-induced proliferation of mouse pancreatic β-cells. To study the effect of HFD on pancreatic β-cell function in mice, their plasma insulin levels were measured in fasting and non-fasting states. HFD-fed mice exhibited hyperinsulinemia and insulin resistance compared with SD-fed mice, while in the HFD-fed mice the serum insulin levels of the AAV-PP2Ac mice were significantly reduced compared with those of the AAV-null mice (Fig. 7A). The western blot analysis of pancreatic tissue revealed that insulin and Pdx1 protein expression was consistent with this (Fig. 7B). Pancreatic tissues ware subjected to staining using insulin antibodies for the identification of β-cells. Evaluation of mouse pancreatic tissue by immunofluorescence showed an increase in the fluorescence intensity of pancreatic β-cells in mice fed with a HFD, while the pancreatic tissue of mice in the AAV-PP2Ac group had a reduced fluorescence intensity compared with that of the AAV-null group for both SD- and HFD-fed mice (Fig. 7C). To further determine the effect of PP2A interference on pancreatic β-cell proliferation, the mouse pancreatic tissue was subjected to Ki67, insulin and DAPI costaining, and the percentage increase

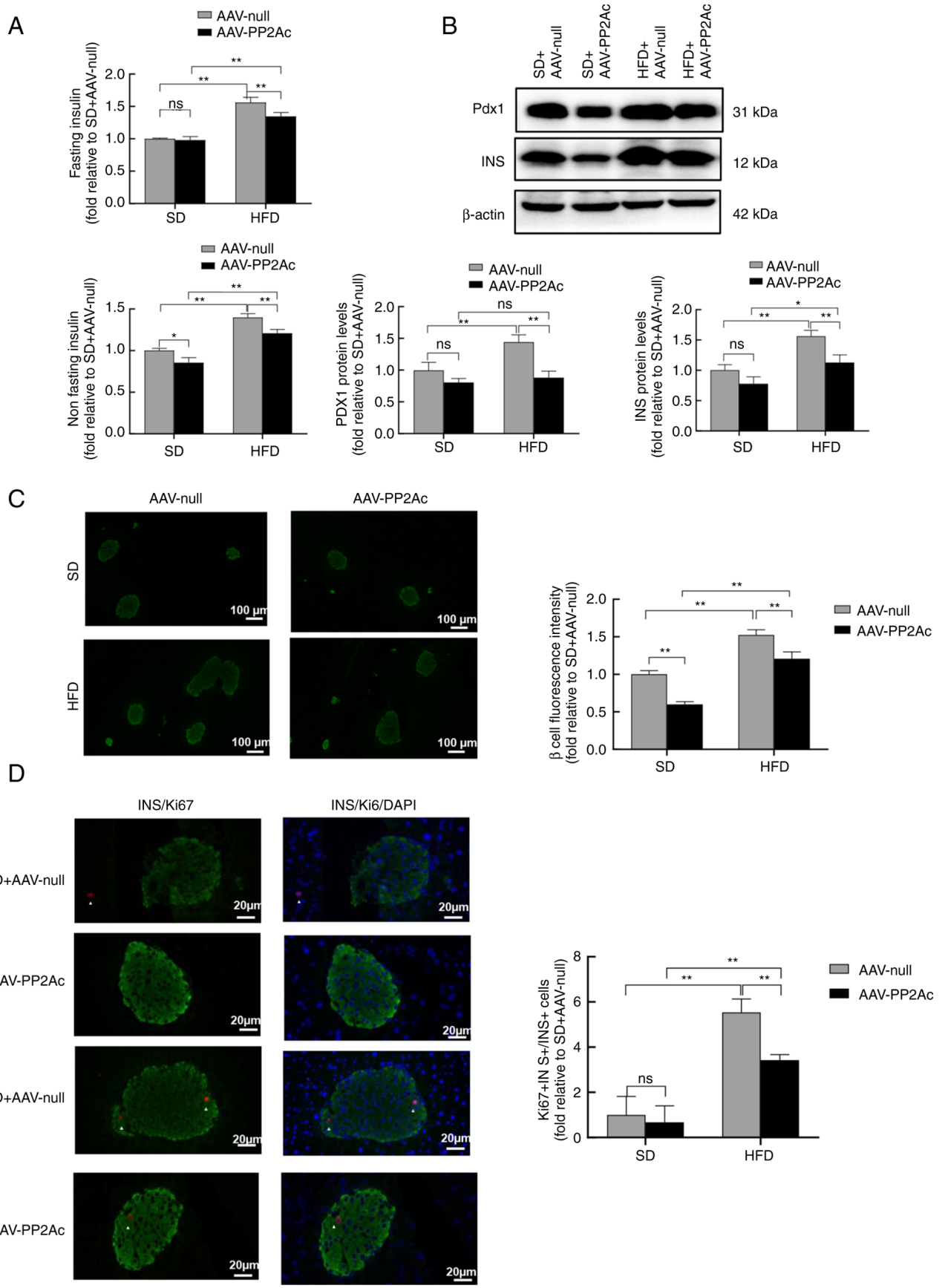

Figure 7. Interfering with PP2Ac attenuates the HFD-induced proliferation of mouse pancreatic β-cells. (A) Measurements of fasting (n=5) and non-fasting (n=3) insulin levels in mouse serum. (B) Protein levels of Pdx1 and INS were analyzed by western blotting (n=3) using β-actin as a loading control. (C) Representative images of the immunofluorescence labeling of pancreatic β-cells (n=6), and quantitative analysis of the fluorescence intensity. (D) Pancreatic β-cell proliferation was calculated using the Ki67 calculation method to determine the percentage of Ki67$^+$ cells among INS$^+$ cells (n=6) using ImageJ software. All experiments were performed at least three times, and values are reported as the mean ± standard deviation. *P<0.05, **P<0.01. PP2Ac, protein phosphatase 2A; AAV, adeno-associated virus; SD, standard diet; HFD, high-fat diet; Pdx1, pancreatic and duodenal homeobox 1; INS, insulin.

in pancreatic β-cell proliferation was calculated. Compared with the low proliferation rate of pancreatic β-cells in mice fed a SD, the β-cells exhibited significantly higher proliferation with a HFD in both AAV-null and AAV-PP2Ac mice, while interfering with PP2Ac gene expression reduced cell proliferation in the HFD-fed mice (Fig. 7D). These findings suggest that the HFD induced compensatory pancreatic β-cell proliferation, the elevation of serum insulin levels and increased insulin resistance in mice, while the reduction of PP2Ac gene expression effectively protected pancreatic tissue against the HFD-induced compensatory proliferation of β-cells.

Discussion

The present study demonstrated that the knockdown of PP2Ac significantly inhibited PP2A activity, attenuated PA-induced ER stress, mitochondrial dysfunction and apoptosis, and increased insulin secretion in MIN6 cells. The specific knockdown of pancreatic PP2Ac protected against insulin resistance and the HFD-induced compensatory proliferation of pancreatic β-cells in mice. Thus, it is hypothesized that PP2Ac may be a novel target for diabetes treatment.

PP2A is a member of the serine/threonine phosphatase family, which accounts for ~1% of total cellular proteins and represents a major class of phosphatases in mammalian cells, the catalytic action of which is mainly attributable to PP2Ac. Two common PP2Ac genotypes, PP2Acα and PP2Acβ, have been reported, and PP2Acα is known to be the major genotype of the two (32). The present study used lentiviral transfection to interfere with PP2Acα gene expression in MIN6 cells. PP2Ac is closely associated with the development of diabetes, heart disease, cancer and neurodegenerative diseases (33). Under glucotoxicity, lipotoxicity and other physiologically stressful conditions, the PP2Ac protein is hyperactivated in the pancreas, liver, muscle, retina and other organs, ultimately leading to the development of insulin resistance and pancreatic β-cell dysfunction. Notably, PP2A activity can be restored to near-normal levels either by interfering with the transcription of the gene encoding PP2Ac or with the expression of PP2Ac protein (24,34,35). The present study found that the HFD feeding of mice and the PA treatment of MIN6 cells induced increases in the PP2A activity of pancreatic β-cells of ~1.8- and 2.6-fold, respectively, during the compensatory and decompensated stages of lipotoxicity. Of note, PP2Ac knockdown reduced PP2A activity and protected pancreatic β-cells. PA is an abundant saturated fatty acid that is involved in the lipotoxicity-induced damage of pancreatic β-cells, which leads to insulin resistance and ultimately, uncompensated T2DM (7,36). In the present study, exposure to a high glucose concentration (20 mM) stimulated MIN6 cells to produce insulin levels much higher than those produced under low glucose conditions (2.5 mM), indicating that the pancreatic β-cells were functioning normally. Treatment with 0.5 mM PA exacerbated apoptosis and inhibited the secretion of insulin in pancreatic β-cells, while interference with PP2Ac expression attenuated the lipotoxicity-induced damage in the MIN6 cells.

The ER and mitochondria are among most important organelles required for pancreatic β-cells to carry out their functions, and they play a crucial role in the synthesis, processing and secretion of insulin (13,14). The two organelles closely interact and form the mitochondria-associated ER membrane, which regulates lipid synthesis and metabolism, the Ca^{2+} signaling pathway, ER stress, mitochondrial function, cell proliferation and apoptosis to maintain cellular stability (37-40). A previous study has shown that PA induces apoptosis via the modulation of multiple pathways, mainly those associated with oxidative stress, ER stress and mitochondrial dysfunction (41). The inhibition of PP2A activity achieved through either a reduction in PP2Ac protein levels or increase in PP2Ac phosphorylation has been shown to attenuate ER stress in hepatocytes subjected to ischemia-reperfusion injury, which is suggested to have the potential to protect donor liver function and improve liver transplant survival (42,43). In the present study, PP2Ac knockdown was indicated to significantly reduce the ER stress caused by PA exposure in MIN6 cells, as the protein levels of CHOP and GRP78 were regulated. In addition, PA exposure has previously been shown to compromise mitochondrial integrity and function, leading to the significant production of ROS and a reduction in the mitochondrial membrane potential (44). PP2Ac knockdown reduced PA-induced ROS levels and attenuated the PA-induced reduction in ATP production, indicating that it attenuated the level of oxidative stress in MIN6 cells. Sustained ER stress and mitochondrial damage eventually lead to apoptosis (10). This is consistent with the observation that increasing either the PA concentration or duration of exposure reduced the viability of MIN6 cells in the present study, and treatment with PA increased the rate of apoptosis, while knocking down PP2Ac reduced the rate of cell death. Therefore, it is speculated that PP2Ac knockdown may reduce the apoptosis of pancreatic β-cells via the attenuation of ER stress and protection of the mitochondrial function in MIN6 cells under lipotoxic conditions.

To investigate the mechanism by which the PP2Ac gene affects MIN6 cell function and apoptosis, RNA sequencing and KEGG pathway enrichment analysis were performed, and the MAPK pathway was selected for immunoblot validation. MAPK family proteins have been shown to be associated with cell proliferation, apoptosis and tumor metastasis, and the main MAPK pathways include ERK, JNK and p38 (45). It has been found that PP2Ac regulates the phosphorylation of proteins in the MAPK signaling pathway and inhibits the migration of cervical cancer cells, while the downregulation of PP2Ac expression increases inflammation in the tumor microenvironment and induces the infiltration and invasion of pancreatic tumors (46,47). These findings suggest that PP2A plays an important role in the inhibition of tumor growth and metastasis and may be a potential target for cancer therapy, while PP2Ac knockdown can inhibit apoptosis under specific circumstances. The results of the present study suggest that knockdown of the PP2Ac gene alleviated the dysfunction and apoptosis of MIN6 cells under lipotoxic conditions by activating the ERK signaling pathway and inhibiting the JNK and p38 pathways.

The current study found that HFD feeding impaired glucose tolerance and induced insulin resistance in C57BL/6 mice, leading to the compensatory proliferation of pancreatic β-cells, but not the decompensated stage. This outcome may be associated with the use of an insufficient feeding duration or the mouse strain that was used. In the cell experiments, after exposure to 0.5 mM PA,

pancreatic β-cells entered the decompensated stage of lipotoxicity. Thus, the animal and cellular experiments in the present effectively demonstrate the role of PP2Ac in pancreatic β-cells throughout the entire process of lipotoxicity. The current study suggested that PP2A activity was much higher in the decompensated stage than in the compensated stage, and that the knockdown of PP2Ac gene expression protected pancreatic β-cells from lipotoxicity throughout the process. Notably, PP2Ac knockdown under normal conditions (without lipotoxicity) has been reported to inhibit GSIS in pancreatic β-cells (48), which may be due to the low level of PP2A activity being insufficient to effectively regulate substrate phosphorylation levels. Therefore, it is hypothesized that the maintenance of PP2A activity at appropriate levels may sustain cellular homeostasis, while excessively high or low levels would be detrimental to cellular function.

In summary, the results of the present study indicate that PP2Ac knockdown attenuated lipotoxicity-induced ER stress and mitochondrial dysfunction in pancreatic β-cells, and protected pancreatic β-cell function, which may have been achieved via the regulation of PP2A activity. The findings provide a solid theoretical basis for the clinical treatment of diabetes and offer new insights for the development of novel drugs targeting PP2Ac in pancreatic β-cells. However, the study has some limitations, as follows: Pancreatic-specific gene knockout mice were not used; only one cell line was used; and the effects of activators and inhibitors of PP2Ac on MIN6 cell function and proliferation apoptosis were not investigated. Therefore, future studies should be designed to overcome these limitations and consolidate the present findings.

Acknowledgements

Not applicable.

Funding

The present study was supported by the National Natural Science Foundation of China (grant no. 81970718).

Availability of data and materials

The RNA sequencing datasets generated and/or analyzed during the current study are available in the GEO repository (https://www.ncbi.nlm.nih.gov/gds/?term=GSE242538). The other datasets used and/or analyzed during the current study are available from the corresponding author on reasonable request.

Authors' contributions

ZZ, BT and YX conceived, designed and carried out the study. JF, LS, HW, JL, CX and MK contributed to performing the experiments. ZZ, JL and BT conducted data analysis and drafted the manuscript. ZZ and YX revised the manuscript. ZZ, BT and YX confirm the authenticity of all the raw data. All authors read and approved the final version of the manuscript.

Ethics approval and consent to participate

The study protocol was approved by The Ethics and Scientific Review Board of the Zhongnan Hospital of Wuhan University (Wuhan, China; approval no. ZN2022037).

Patient consent for publication

Not applicable.

Competing interests

The authors declare that they have no competing interests.

References

1. Amanat S, Ghahri S, Dianatinasab A, Fararouei M and Dianatinasab M: Exercise and type 2 diabetes. Adv Exp Med Biol 1228: 91-105, 2020.
2. Sun H, Saeedi P, Karuranga S, Pinkepank M, Ogurtsova K, Duncan BB, Stein C, Basit A, Chan JCN, Mbanya JC, *et al*: IDF Diabetes atlas: Global, regional and country-level diabetes prevalence estimates for 2021 and projections for 2045. Diabetes Res Clin Pract 183: 109119, 2022.
3. Xiong QY, Yu C, Zhang Y, Ling L, Wang L and Gao JL: Key proteins involved in insulin vesicle exocytosis and secretion. Biomed Rep 6: 134-139, 2017.
4. Rutter GA, Pullen TJ, Hodson DJ and Martinez-Sanchez A: Pancreatic β-cell identity, glucose sensing and the control of insulin secretion. Biochem J 466: 203-218, 2015.
5. Zheng Y, Ley SH and Hu FB: Global aetiology and epidemiology of type 2 diabetes mellitus and its complications. Nat Rev Endocrinol 14: 88-98, 2018.
6. Klein S, Gastaldelli A, Yki-Järvinen H and Scherer PE: Why does obesity cause diabetes? Cell Metab 34: 11-20, 2022.
7. Oh YS, Bae GD, Baek DJ, Park EY and Jun HS: Fatty acid-induced lipotoxicity in pancreatic beta-cells during development of type 2 diabetes. Front Endocrinol (Lausanne) 9: 384, 2018.
8. Ertunc ME and Hotamisligil GS: Lipid signaling and lipotoxicity in metaflammation: Indications for metabolic disease pathogenesis and treatment. J Lipid Res 57: 2099-2114, 2016.
9. Ron D and Walter P: Signal integration in the endoplasmic reticulum unfolded protein response. Nat Rev Mol Cell Biol 8: 519-529, 2007.
10. Lin S, Long H, Hou L, Zhang M, Ting J, Lin H, Zheng P, Lei W, Yin K and Zhao G: Crosstalk between endoplasmic reticulum stress and non-coding RNAs in cardiovascular diseases. Wiley Interdiscip Rev RNA 14: e1767, 2022.
11. Hamacher-Brady A and Brady NR: Mitophagy programs: Mechanisms and physiological implications of mitochondrial targeting by autophagy. Cell Mol Life Sci 73: 775-795, 2016.
12. Roszczyc-Owsiejczuk K and Zabielski P: Sphingolipids as a culprit of mitochondrial dysfunction in insulin resistance and type 2 diabetes. Front Endocrinol (Lausanne) 12: 635175, 2021.
13. Thivolet C, Vial G, Cassel R, Rieusset J and Madec AM: Reduction of endoplasmic reticulum-mitochondria interactions in beta cells from patients with type 2 diabetes. PLoS One 12: e0182027, 2017.
14. Ježek P, Holendová B, Jabůrek M, Dlasková A and Plecitá-Hlavatá L: Contribution of mitochondria to insulin secretion by various secretagogues. Antioxid Redox Signal 36: 920-952, 2022.
15. Carta G, Murru E, Banni S and Manca C: Palmitic acid: Physiological role, metabolism and nutritional implications. Front Physiol 8: 902, 2017.
16. Lytrivi M, Castell AL, Poitout V and Cnop M: Recent insights into mechanisms of β-cell Lipo- and glucolipotoxicity in type 2 diabetes. J Mol Biol 432: 1514-1534, 2020.
17. Raman D and Pervaiz S: Redox inhibition of protein phosphatase PP2A: Potential implications in oncogenesis and its progression. Redox Biol 27: 101105, 2019.
18. Reynhout S and Janssens V: Physiologic functions of PP2A: Lessons from genetically modified mice. Biochim Biophys Acta Mol Cell Res 1866: 31-50, 2019.

19. Ronk H, Rosenblum JS, Kung T and Zhuang Z: Targeting PP2A for cancer therapeutic modulation. Cancer Biol Med 19: 1428-1439, 2022.
20. Binder P, Wang S, Radu M, Zin M, Collins L, Khan S, Li Y, Sekeres K, Humphreys N, Swanton E, *et al*: Pak2 as a novel therapeutic target for cardioprotective endoplasmic reticulum stress response. Circ Res 124: 696-711, 2019.
21. Yang L, Jin GH and Zhou JY: The role of ceramide in the pathogenesis of alcoholic liver disease. Alcohol Alcohol 51: 251-257, 2016.
22. Theurey P, Tubbs E, Vial G, Jacquemetton J, Bendridi N, Chauvin MA, Alam MR, Le Romancer M, Vidal H and Rieusset J: Mitochondria-associated endoplasmic reticulum membranes allow adaptation of mitochondrial metabolism to glucose availability in the liver. J Mol Cell Biol 8: 129-143, 2016.
23. Chen X, Chen S, Shen T, Yang W, Chen Q, Zhang P, You Y, Sun X, Xu H, Tang Y, *et al*: Adropin regulates hepatic glucose production via PP2A/AMPK pathway in insulin-resistant hepatocytes. FASEB J 34: 10056-10072, 2020.
24. Arora DK, Machhadieh B, Matti A, Wadzinski BE, Ramanadham S and Kowluru A: High glucose exposure promotes activation of protein phosphatase 2A in rodent islets and INS-1 832/13 β-cells by increasing the posttranslational carboxylmethylation of its catalytic subunit. Endocrinology 155: 380-391, 2014.
25. Livak KJ and Schmittgen TD: Analysis of relative gene expression data using real-time quantitative PCR and the 2(-Delta Delta C(T)) method. Methods 25: 402-408, 2001.
26. Li Y, Zhang QY, Sun BF, Ma Y, Zhang Y, Wang M, Ma C, Shi H, Sun Z, Chen J, *et al*: Single-cell transcriptome profiling of the vaginal wall in women with severe anterior vaginal prolapse. Nat Commun 12: 87, 2021.
27. Kanehisa M: Toward understanding the origin and evolution of cellular organisms. Protein Sci 28: 1947-1951, 2019.
28. Dong WW, Feng Z, Zhang YQ, Ruan ZS and Jiang L: Potential mechanism and key genes involved in mechanical ventilation and lipopolysaccharide-induced acute lung injury. Mol Med Rep 22: 4265-4277, 2020.
29. Deng S, Yang L, Ma K and Bian W: Astragalus polysaccharide improve the proliferation and insulin secretion of mouse pancreatic β-cells induced by high glucose and palmitic acid partially through promoting miR-136-5p and miR-149-5p expression. Bioengineered 12: 9872-9884, 2021.
30. Wee J, Pak S, Kim T, Hong GS, Lee JS, Nan J, Kim H, Lee MO, Park KS and Oh U: Tentonin 3/TMEM150C regulates glucose-stimulated insulin secretion in pancreatic β-cells. Cell Rep 37: 110067, 2021.
31. Zhang Y, Yang X, Ge X and Zhang F: Puerarin attenuates neurological deficits via Bcl-2/Bax/cleaved caspase-3 and Sirt3/SOD2 apoptotic pathways in subarachnoid hemorrhage mice. Biomed Pharmacother 109: 726-733, 2019.
32. Janssens V and Goris J: Protein phosphatase 2A: A highly regulated family of serine/threonine phosphatases implicated in cell growth and signalling. Biochem J 353: 417-439, 2001.
33. Baskaran R and Velmurugan BK: Protein phosphatase 2A as therapeutic targets in various disease models. Life Sci 210: 40-46, 2018.
34. Kowluru A and Matti A: Hyperactivation of protein phosphatase 2A in models of glucolipotoxicity and diabetes: Potential mechanisms and functional consequences. Biochem Pharmacol 84: 591-597, 2012.
35. Kowluru A: Potential roles of PP2A-Rac1 signaling axis in pancreatic β-cell dysfunction under metabolic stress: Progress and promise. Biochem Pharmacol 180: 114138, 2020.
36. Acosta-Montaño P and García-González V: Effects of dietary fatty acids in pancreatic beta cell metabolism, implications in homeostasis. Nutrients 10: 393, 2018.
37. Madec AM, Perrier J, Panthu B and Dingreville F: Role of mitochondria-associated endoplasmic reticulum membrane (MAMs) interactions and calcium exchange in the development of type 2 diabetes. Int Rev Cell Mol Biol 363: 169-202, 2021.
38. Lee S and Min KT: The interface between ER and mitochondria: Molecular compositions and functions. Mol Cells 41: 1000-1007, 2018.
39. Szymański J, Janikiewicz J, Michalska B, Patalas-Krawczyk P, Perrone M, Ziółkowski W, Duszyński J, Pinton P, Dobrzyń A and Więckowski MR: Interaction of mitochondria with the endoplasmic reticulum and plasma membrane in calcium homeostasis, lipid trafficking and mitochondrial structure. Int J Mol Sci 18: 1576, 2017.
40. Tubbs E and Rieusset J: Metabolic signaling functions of ER-mitochondria contact sites: Role in metabolic diseases. J Mol Endocrinol 58: R87-R106, 2017.
41. Xu D, Liu L, Zhao Y, Yang L, Cheng J, Hua R, Zhang Z and Li Q: Melatonin protects mouse testes from palmitic acid-induced lipotoxicity by attenuating oxidative stress and DNA damage in a SIRT1-dependent manner. J Pineal Res 69: e12690, 2020.
42. Lan J, Zhong Z, Wang Y, Xiong Y and Ye Q: Endoplasmic reticulum stress induces liver cells apoptosis after brain death by suppressing the phosphorylation of protein phosphatase 2A. Mol Med Rep 21: 567-574, 2020.
43. Xiong Y, Lan J, Huang K, Zhang Y, Zheng L, Wang Y and Ye Q: PP2Ac upregulates PI3K-Akt signaling and induces hepatocyte apoptosis in liver donor after brain death. Apoptosis 24: 921-933, 2019.
44. Li N, Frigerio F and Maechler P: The sensitivity of pancreatic beta-cells to mitochondrial injuries triggered by lipotoxicity and oxidative stress. Biochem Soc Trans 36: 930-934, 2008.
45. Sui X, Kong N, Ye L, Han W, Zhou J, Zhang Q, He C and Pan H: p38 and JNK MAPK pathways control the balance of apoptosis and autophagy in response to chemotherapeutic agents. Cancer Lett 344: 174-179, 2014.
46. Zheng HY, Shen FJ, Tong YQ and Li Y: PP2A Inhibits cervical cancer cell migration by dephosphorylation of p-JNK, p-p38 and the p-ERK/MAPK signaling pathway. Curr Med Sci 38: 115-123, 2018.
47. Tao M, Liu L, Shen M, Zhi Q, Gong FR, Zhou BP, Wu Y, Liu H, Chen K, Shen B, *et al*: Inflammatory stimuli promote growth and invasion of pancreatic cancer cells through NF-κB pathway dependent repression of PP2Ac. Cell Cycle 15: 381-393, 2016.
48. Jangati GR, Veluthakal R, Susick L, Gruber SA and Kowluru A: Depletion of the catalytic subunit of protein phosphatase-2A (PP2Ac) markedly attenuates glucose-stimulated insulin secretion in pancreatic beta-cells. Endocrine 31: 248-253, 2007.